Surface-Melting Transitions and Phase Coexistence in Argon Solvent Clusters

Jürg Bösiger and Samuel Leutwyler
Institut für Anorganische, Analytische und Physikalische Chemie, CH-3000 Bern 9, Switzerland
(Received 14 April 1987)

Electronic spectra of carbazole·Ar_n clusters in supersonic beams exhibit specific size-dependent spectral features, showing only sharp intermolecular vibrational bands for $n=1$ to 3, both broad and narrow spectral bands for $n=4$ to 6, and only broad bands for $n \geq 7$. Monte Carlo simulations indicate that the change from sharp to broad structure is due to surface-melting transitions of the solvent clusters relative to the substrate, and predict a finite-width solidlike-liquidlike coexistence range in agreement with the experimental observations.

PACS numbers: 36.40.+d, 33.10.Gx

The study of melting transitions in clusters and small particles is important for a deeper microscopic understanding of the solid $\leftrightarrow$ liquid phase transition. Two main points are of interest: (1) the size dependence of the melting transition temperature and (2) the width and shape of the transition in finite systems. The melting points of small particles have long been predicted to decrease with decreasing particle size.[1] Several molecular-dynamics (MD) and Monte Carlo (MC) simulation studies on Ar_n clusters ($n=3$–100) have found size-dependent and sharp melting transitions.[2–5] However, Berry, Jellinek, and Natanson have predicted by quantum-statistical model calculations that clusters should show unequal freezing and melting temperatures T_f and T_m and a coexistence range (T_f, T_m) over which both solidlike and liquidlike forms should coexist.[6,7] This prediction is supported by an MD study on Ar_{13}.[8]

Experimental information is still sparse: Melting-point measurements of supported Pb, Sn, Bi, In, and Au particles agree well with the Pawlow equation[1] down to sizes of 10 Å.[9–13] Infrared photodepletion spectroscopic measurements of SF_6-Ar_n clusters performed by Gough, Knight, and Scoles[14] have been interpreted by Eichenauer and LeRoy[15] in terms of cluster structures involving "surface" and "surrounded" SF_6 chromophores. A recent reexamination of the synthetic spectra by MD calculations[16] has, however, led to a reinterpretation in terms of Ar-coverage–dependent splitting of the triply degenerate ν_3 band of SF_6.

We have measured the electronic spectra of carbazole·Ar_n rare-gas solvent clusters with $n=1$–35, by resonant two-photon ionization (R2PI) spectroscopy with mass-spectrometric detection, at the near-uv transition $S_1 \leftarrow S_0$ ($^1A_1 \leftarrow {}^1A_1$) of the carbazole substrate molecule. Since cluster fragmentation can be shown to be negligible under carefully controlled conditions,[17,18] cluster sizes are unequivocally determined, and species-specific electronic spectra are obtained. The molecular-beam apparatus and time-of-flight mass spectrometer have been previously described.[16,17] The rare-gas solvent clusters were formed by adiabatic expansion of carbazole at a vapor pressure of 0.1–0.3 mbar, seeded in Ar (25 at.%)/Ne (75 at.%) carrier gas through a pulsed circular 0.5-mm-diam nozzle ($T_0=395$ K, $p_0=1.2$–2.0 bars).

The R2PI spectra of the carbazole·Ar_n clusters with $n=1$–8 are highly individual; see Figs. 1(a) and 1(b). The following points are especially relevant here: (1) Clusters with $n=1$–6 exhibit sharp electronic origins followed, towards higher frequencies, by vibrational bands which correspond to intermolecular carbazole-Ar_n vibrations in the S_1 state. These observations imply the existence of (a) single predominant cluster structures and (b) well-defined solvent cluster vibrations. (2) At $n=4$, an additional broad, red-shifted, smooth band appears about 60 cm^{-1} to the red of the 0_0^0 transition, extending into the region of sharp spectral bands. The MC simulations presented below show that the solvent clusters with $n \geq 4$ exhibit a *surface-melting transition* at temperatures above 14–18 K; the resulting frequency spectrum of the intermolecular motions is expected to be quasicontinuous, in agreement with the observed band shape. (3) Clusters with $n=4$–6 show discrete peaks and broad, diffuse bands simultaneously, suggesting that localized and disordered, fluxional structures coexist in this size range. (4) For $n=7$ and larger, the sharp bands disappear altogether, and only broad structures remain [Fig. 1(b)], implying that the larger clusters have undergone complete surface melting.

Both MD and MC calculations were performed on the carbazole·Ar_n clusters. These indicate that the trends in spectral band shapes described above are due to the uncoupling of the motions of the solvent cluster from the substrate molecule, which takes place over a finite temperature range. The intermolecular potential energy was modeled with an atom-atom potential which has previously been shown to yield near-quantitative results for structural and energetic properties of aromatic-molecule/rare-gas van der Waals complexes.[19–22]. The Lennard-Jones 12-6 potential parameters were $\epsilon_{Ar\text{-}C}=61.923$ K, $\epsilon_{Ar\text{-}H}=42.768$ K, $\epsilon_{Ar\text{-}Ar}=142.1$ K, and $\sigma_{Ar\text{-}C}=3.3854$ Å, $\sigma_{Ar\text{-}H}=3.2072$ Å, $\sigma_{Ar\text{-}Ar}=3.36$ Å. As a starting point for the MC calculations, minimum-

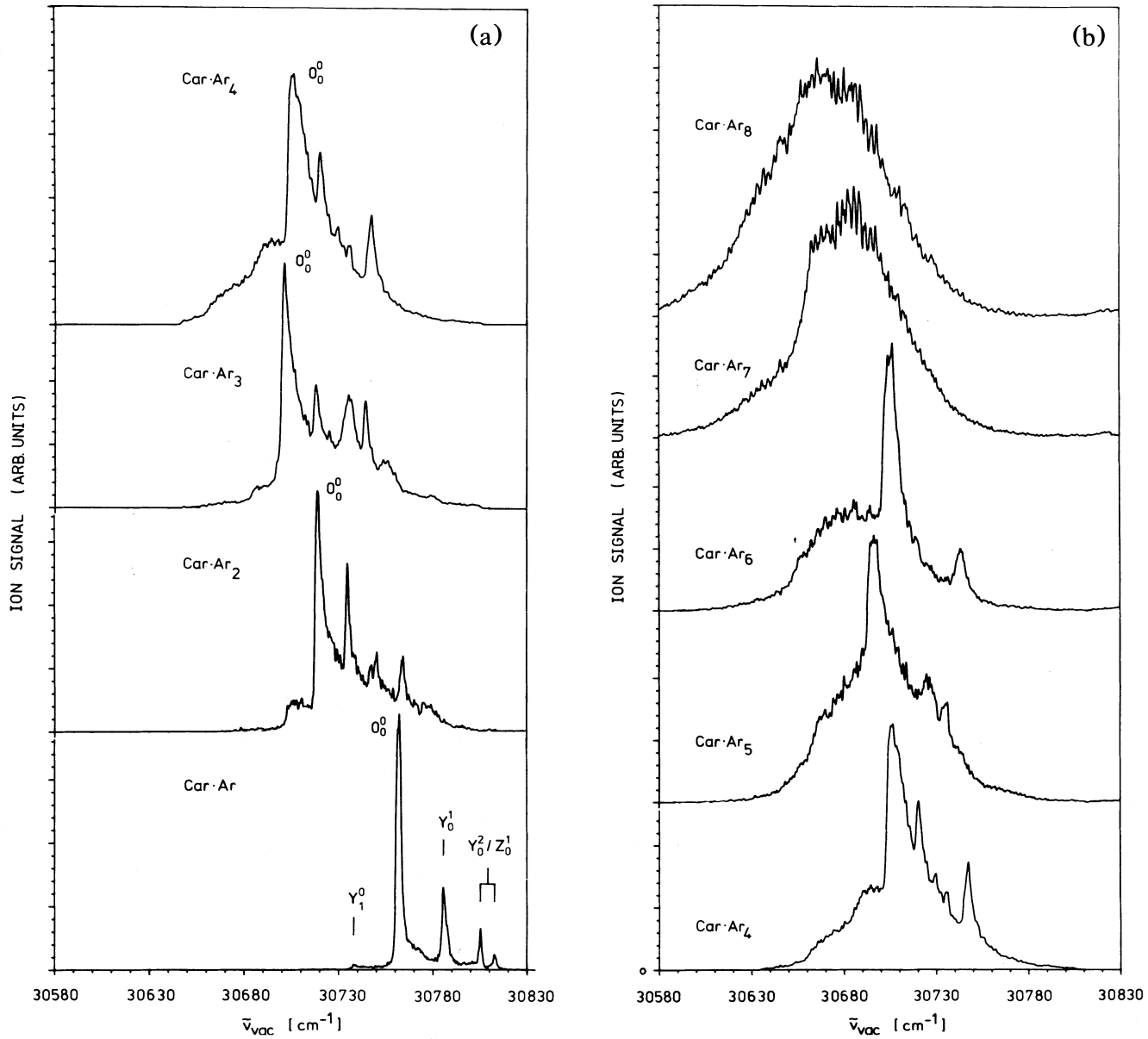

FIG. 1. (a) R2PI spectra of carbazole·Ar_n ($n=1-4$) in the region of the $S_1 \leftarrow S_0$ origins (marked as 0_0^0). The bare carbazole electronic origin (not shown) is at 30809 cm^{-1}. The weak excitations to the high-frequency side are intermolecular carbazole$\leftrightarrow Ar_n$ vibrations; two short-axis excitations (Y_0^1 and Y_0^2) and an out-of-plane excitation (Z_0^1) are assigned for $n=1$. Note the diffuse, red-shifted spectral feature in the $n=4$ spectrum. (b) Same for $n=4-8$. Note the continuous increase of the intensity of the broad, diffuse spectral features relative to the sharp spectral features for $n=4-6$. For $n=7$ and 8, the sharp features disappear completely and only the broad features remain.

energy solvent cluster structures were determined for $n=1-7$ by slow cooling in the molecular-dynamics simulation. Varying the time steps from 1×10^{-14} to 5×10^{-14} s had no influence on the resulting structures. The minimum-energy structures found by the MD simulations are all "same sided", with the solvent cluster forming a continuous two-dimensionally close-packed structure covering the central part of one surface of the substrate. A single energetically low-lying structure was found for $n=1-3$. The larger clusters exhibit many distinct isomers: The number of isomers within 50 cm^{-1} of the absolute energy minimum (not counting enantiomers) is 2, 7, 7, and 1 for $n=4$, 5, 6, and 7, respectively. The appearance of energetically low-lying structural isomers with increasing cluster size is suggestive of a heterogeneous spectral broadening mechanism; however,

the 0-K structure calculations predict heterogeneous broadening to be moderate for $n=4$, important for $n=5$ and 6, but unimportant for $n=7$, which is in disagreement with the experimental observations.

Cluster phase transitions were investigated by the Metropolis MC simulation technique with the same potential as for the MD calculations. Initial equilibrations were performed for 1×10^5 to 2×10^5 steps, and results were recorded for 5×10^5 to 2×10^6 steps. Since our interest is mainly in the structural transitions of the solvent clusters, we have evaluated (a) the spatial distribution functions of the Ar atoms relative to the carbazole-substrate frame $\rho_i=\rho(\{\mathbf{r}_i\};T)$, $i=1,\ldots,n$; (b) the standard deviation of the atomic position vector of the ith Ar adatom, σ_1, relative to the carbazole center of mass, which characterizes the *rigidity of the Ar cluster relative to the substrate frame;* and (c) the normalized root mean square Ar-Ar bond length fluctuation

$$\delta(d_{ij})=\{\langle d_{ij}^2\rangle-\langle d_{ij}\rangle^2\}^{1/2}/\langle d_{ij}\rangle$$

between Ar atoms i and j, which characterizes the *internal rigidity of the solvent cluster.* Four qualitatively distinct order-disorder or phase transitions were found; in order of rising temperature, these are (1) surface isomerization transitions, (2) cluster rigid-fluxional transitions, (3) surface-melting transitions, and (4) cluster-melting transitions. At the isomerization transitions, interconversion takes place between different isomers (for $n=6$) or enantiomers (for $n=4$–7). Isomerization is characterized by steplike increases of several σ_i values. Since the transition interconverts mirror-symmetric forms, the spectroscopic changes accompanying the transition should be barely observable, with a possible exception at $n=6$. At the rigid-fluxional transition temperatures, the solvent clusters undergo structural changes which involve some, but not all, intracluster Ar—Ar bonds, accompanied by steplike increases in the corresponding δ_{ij} values. Surface-melting transitions are fairly gradual, taking place over several degrees, and are characterized by increases in *all* of the σ_i values from $\sigma_i\leq0.6$ Å at the lower end (freezing temperature) to $\sigma_j\geq1.8$ Å at the upper end of the transition range (melting temperature). The transition ranges are 14–19 K ($n=4$), 16–19 K ($n=5$), and 18–21 K ($n=6$ and 7). For large fractions of the Markov chain (up to 5×10^5 steps) the solvent cluster exhibits either a localized or a fluxional structure with respect to the substrate, the two interconverting by a series of surface rotational/translational hops. This behavior is typical for all solvent clusters with $n=4$–7 over the surface-melting transition range. Although some intracluster structural rearrangements occur, the solvent cluster itself is *not* liquidlike, since the large majority of the intracluster bonds remain stiff, with $\delta_{ij}<10\%$, up to 25–30 K.

Because the electronic transition is localized in the carbazole molecule, the main factor influencing the width and shape of the electronic-vibrational bands is the adatom positional distribution relative to the substrate molecule. The surface-melting transitions dramatically expand the region of configuration space accessible to the solvent clusters, resulting in a smearing of the positional distributions of the adatoms and a broadening of the electronic transition. In addition, new low-frequency vibrational modes appear, which may couple to the electronic transition.

The internal temperatures of the $n=1$–3 clusters can be determined by hot bands appearing on the low-frequency side of the 0_0^0 transitions: Approximate vibrational temperatures are 11 ± 2 K ($n=1$), 14 ± 2 K ($n=2$), and 15 ± 3 K ($n=3$). Extrapolating linearly to higher n, we estimate internal temperatures in the range $T_{\text{vib}}=16$–22 K for $n=4$–7. The observed and extrapolated vibrational temperatures together with the calculated ranges for the surface-melting transitions for $n=1$–7 are plotted in Fig. 2. For $n=2$ and 3, the internal temperatures are below the surface-melting temperatures, which are sharp for these two clusters. However, for $n=4$–6, the internal temperatures are estimated to lie within, and for $n=7$, slightly above, the surface-melting temperature range. These trends parallel the qualitative behavior exhibited in Figs. 1(a) and 1(b): Solvent clusters that are below the surface freezing point show sharp bands, clusters with internal temperatures falling inside the surface-melting temperature range exhibit both broad and sharp bands simultaneously, and the clusters with internal temperatures above the surface-melting point show only a broad band contour. Thus, the calculations provide strong support for the interpretation of the spectral band shapes in terms of solvent-cluster surface-melting transitions with coexistence ranges of finite width. Classical simulations of

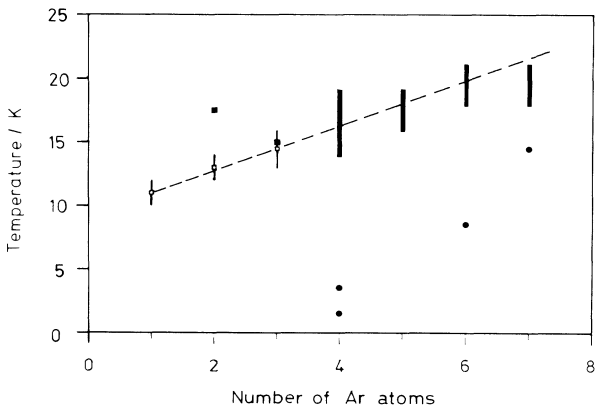

FIG. 2. Comparison of calculated surface-melting temperatures or melting temperature ranges (filled squares or vertical bars), with experimental vibrational temperatures (open squares) for carbazole·Ar_n ($n=1$–3), extrapolated to $n=7$ (dashed line). Also included are the calculated isomerization temperatures (filled circles).

the electronic band shapes, which are currently in progress, also support this interpretation.

While we feel that the consistency of the theoretical predictions with the experimental data is very good, we cannot completely rule out alternative interpretations, given the approximate nature of the model potentials and the uncertainties attached to the experimental temperatures. The model potentials can be improved by inclusion of substrate→cluster induced-multipole, Ar-Ar induced multipole–induced multipole, and three-body interactions.[23] Experimentally, it will be interesting to investigate further the question of homogeneous versus inhomogeneous contributions to the broad and diffuse bands by hole-burning and laser fluorescence line-narrowing techniques.

We thank Dr. R. Bombach for performing the MD structure minimizations. This work was supported by the Schweizerische Nationalfonds under Grants No. 2.688-0.85 and No. 2.065-0.86.

[1]P. Pawlow, Z. Phys. Chem. **65**, 1 (1909).

[2]R. D. Etters and J. B. Kaelberer, Phys. Rev. A **11**, 1068 (1975), and J. Chem. Phys. **66**, 5112 (1977).

[3]J. B. Kaelberer and R. D. Etters, J. Chem. Phys. **66**, 3233 (1977).

[4]C. L. Briant and J. J. Burton, J. Chem. Phys. **63**, 2045 (1975).

[5]N. Quirke and P. Sheng, Chem. Phys. Lett. **110**, 63 (1984).

[6]R. S. Berry, J. Jellinek, and G. Natanson, Chem. Phys. Lett. **107**, 227 (1984).

[7]R. S. Berry, J. Jellinek, and G. Natanson, Phys. Rev. A **30**, 919 (1984).

[8]J. Jellinek, T. L. Beck, and R. S. Berry, J. Chem. Phys. **84**, 2783 (1986).

[9]M. Takagi, J. Phys. Soc. Jpn. **9**, 359 (1954).

[10]C. J. Coombes, J. Phys. F **2**, 441 (1972).

[11]Gl. S. Zhdanov, Kristallografiya **21**, 1220 (1976) [Sov. Phys. Crystallogr. **21**, 706 (1976).

[12]P. Buffat and J.-P. Borel, Phys. Rev. A **13**, 2287 (1976).

[13]J.-P. Borel, Surf. Sci. **106**, 1 (1981).

[14]T. E. Gough, D. G. Knight, and G. Scoles, Chem. Phys. Lett. **97**, 155 (1983).

[15]D. Eichenauer and R. J. LeRoy, Phys. Rev. Lett. **57**, 2920 (1986).

[16]R. J. LeRoy, J. C. Shelley, and D. Eichenauer, in Proceedings of the Twentieth Jerusalem Symposium on Large Finite Systems, edited by J. Jortner (Reidel, Dordrecht, to be published).

[17]E. Honegger, R. Bombach, and S. Leutwyler, J. Chem. Phys. **85**, 1234 (1986).

[18]O. Cheshnovsky and S. Leutwyler, Chem. Phys. Lett. **121**, 1 (1985).

[19]M. J. Ondrechen, Z. Berkovitch-Yellin, and J. Jortner, J. Am. Chem. Soc. **103**, 6586 (1981).

[20]U. Even, A. Amirav, S. Leutwyler, M. J. Ondrechen, Z. Berkovitch-Yellin, and J. Jortner, Faraday Discuss. Chem. Soc. **73**, 153 (1982).

[21]S. Leutwyler, A. Schmelzer, and R. Meyer, J. Chem. Phys. **79**, 4385 (1983).

[22]S. Leutwyler, J. Chem. Phys. **81**, 5480 (1984).

[23]J. Bösiger and S. Leutwyler, to be published.